Journal of Catalysis 268 (2009) iii–viii

Contents lists available at ScienceDirect

Journal of Catalysis

journal homepage: www.elsevier.com/locate/jcat

Journal of Catalysis Vol. 268, Issue 2, 2009

Contents

REGULAR ARTICLES

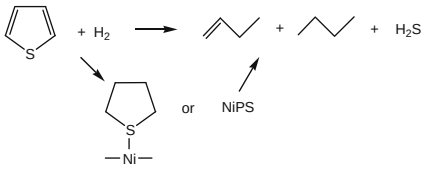

In situ infrared spectroscopy during hydrodesulfurization of thiophene over Ni_2P/MCM-41 showed the presence of tetrahydrothiophene, while transient X-ray absorption spectroscopy showed a Ni–S bond due to this species or a phosphosulfide.

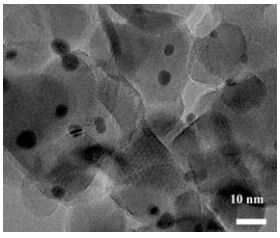

m-Dinitrobenzene hydrogenation over Au/TiO_2 (see TEM image) exhibited a particle size sensitivity delivering higher specific rates over smaller Au particle sizes (in the range 3.4–10.0 nm), irrespective of support anatase:rutile ratio; Au particles <5 nm favour partial – NO_2 reduction to generate *m*-nitroaniline, a response that is linked to Au electronic character, which impacts on *m*-dinitrobenzene adsorption/activation.

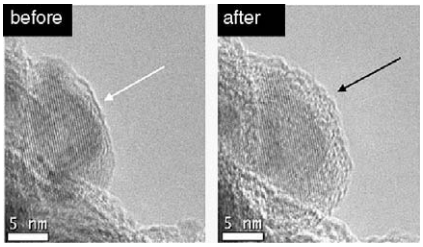

An important issue in iron-based Fischer–Tropsch catalysts is its air-sensitivity. Using both XRD and TEM-EELS in quasi in situ mode, we found that carbon is freed from iron carbides during exposure to air and deposited as a separate amorphous phase. When studying these catalysts, exposure to air should be avoided completely.

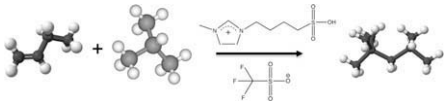

Mixtures of ionic liquids (with acidity manifested in the cation and/or anion) and conventional acids display tunable synergy and offer superior conversion, selectivity, and catalyst stability for the title reaction.

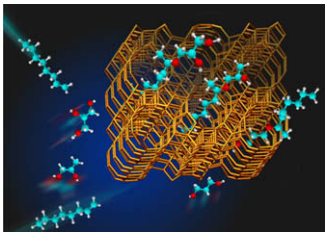

Direct etherification of biomass-based alcohols with 1-octene can be performed over solid acid catalysts such as zeolite Beta as a new route for synthesis of the valuable long alkyl chain ethers with very high selectivities.

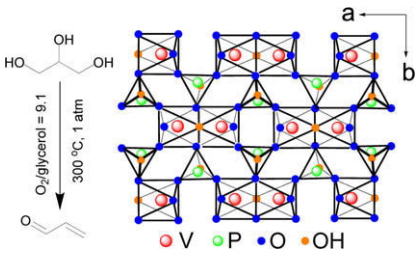

Catalysts of vanadium phosphate oxides were studied in glycerol dehydration to acrolein in the temperature range of 250–350 °C with an O_2/glycerol ratio of 0–13.6.

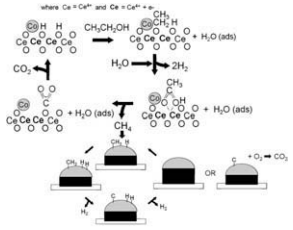

A reaction mechanism was proposed based on in situ DRIFTS and ethanol TPD. Reaction type, feed ratio, and temperature influence amounts and types of carbon deposited and in turn, catalyst stability.

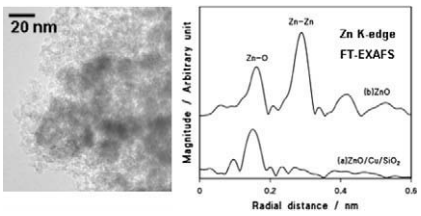

By-production of CO in methanol steam reforming to H_2 and CO_2 is significantly suppressed by the addition of ZnO to Cu/SiO_2 prepared by a sol–gel method. ZnO is highly dispersed in the catalyst.

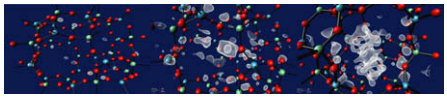

In situ X-ray diffraction and Raman investigations of SAPO-34 during methanol-to-olefin conversion show asymmetric expansion of the catalyst linked to the build-up of intermediates in the zeolite cages.

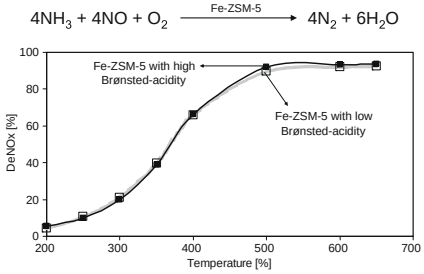

The selective catalytic reduction of NO with NH_3 has been studied over Fe-ZSM-5 samples with equal exchange degrees and active sites but different Brønsted-acidities. The experiments revealed that the acidity of the catalyst is not a crucial factor for high activity and that Brønsted-acidity may not be required for adsorbing or activating the ammonia.

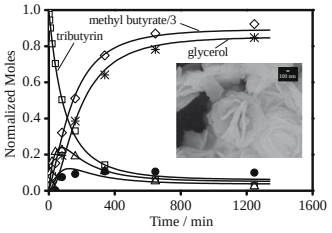

Variations in the textural properties of reconstructed hydrotalcites did not significantly affect the surface base site density or turnover rate of tributyrin transesterification with methanol. However, trace water enhanced the rate of transesterification and promoted severe catalyst deactivation by hydrolysis.

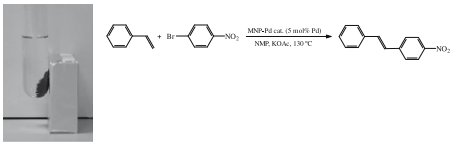

The kinetics of C–C coupling reactions and hydrogenation were studied to investigate the reactivity and separation effectiveness of palladium-based magnetic nanocatalysts.

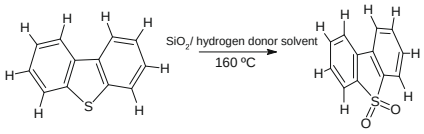

We present a process for oxidizing dibenzothiophene (DBT) to dibenzothiophene-sulfone (DBT-sulfone) using silica gel in the presence of a hydrogen donor solvent where no oxidizing agent was necessary.

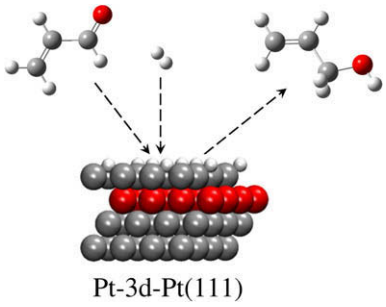

Pt–3d–Pt(1 1 1) structures, where 3d = Ni or Co, are shown to have increased activity for the selective hydrogenation of the C=O bond of acrolein.

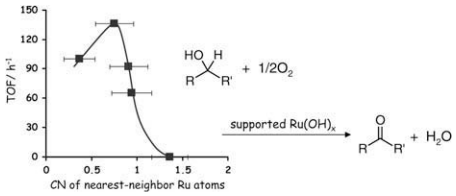

The supported $Ru(OH)_x$ catalysts could act as efficient heterogeneous catalysts for the aerobic oxidation alcohols. The present oxidation was dependent on the coordination number of nearest-neighbor Ru atoms.

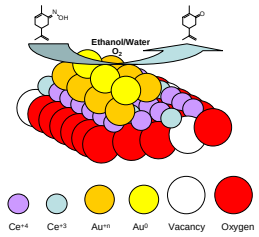

Aliphatic and aromatic oximes, including carvoxime, can be converted into the corresponding ketones and aldehydes using oxygen as a reagent and gold nanoparticles supported on nanoparticulated ceria as catalysts.

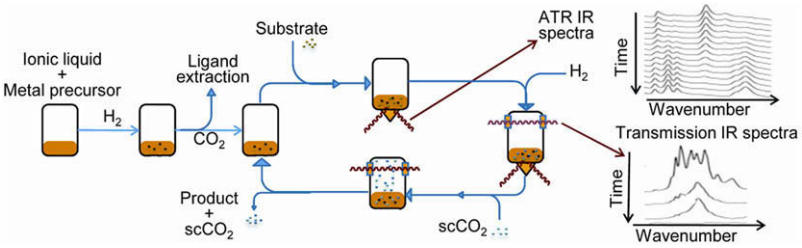

Palladium and Rhodium nanoparticles were synthesized in different ionic liquids and subsequently used as catalysts in solventless hydrogenations. Supercritical carbon dioxide served for the removal of metal precursor ligands and product extraction.

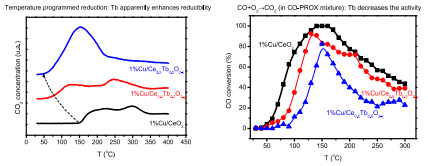

Reasons for the discrepancies between redox and catalytic properties on the basis of classical CO temperature-programmed reduction tests starting at room temperature are explored in $Ce_{1-x}Tb_xO_{2-y}$-supported copper catalysts by *in situ* infrared.

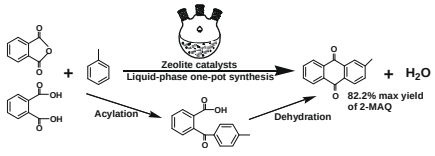

Liquid-phase cascade acylation/dehydration promoted by H-beta zeolite is an effectual strategy to yield 2-methylanthraquinone in 82.2%. The acidity and morphology strongly affect catalytic properties and coke formation.

RESEARCH NOTE

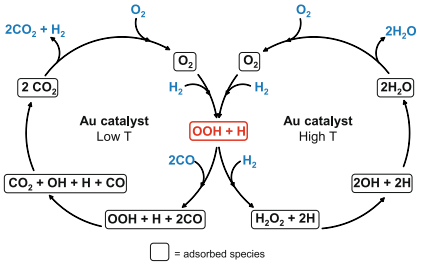

H_2 promotes low-temperature CO oxidation on gold via the formation of hydroperoxy intermediates, also present in hydrogen oxidation.